Experimental Mechanics (2014) 54:501–514
DOI 10.1007/s11340-013-9811-9

Characterization of the Orthotropic Elastic Constants of a Micronic Woven Wire Mesh via Digital Image Correlation

S.M. Kraft · F.A. Moslehy · Y. Bai · A.P. Gordon

Received: 10 July 2012 / Accepted: 13 September 2013 / Published online: 14 November 2013

Abstract Woven structures are steadily emerging as excellent reinforcing components in dual-phase composite materials subjected to multiaxial loads, thermal shock, and aggressive reactants in the environment. Metallic woven wire mesh materials in particular display good ductility and relatively high specific strength and specific resilience. While use of this class of materials is rapidly expanding, a significant gap in property characterization remains. This research classifies the homogenized, orthotropic material properties of a representative twill dutch woven wire mesh through the use of in-plane uniaxial tensile experiments incorporating a Digital Image Correlation (DIC) strain measurement technique. Values for elastic modulus and Poisson's ratio are calculated from the experimental data, and shear modulus values are identified by means of constitutive modeling. This approach establishes a reproducible method for characterizing the in-plane elastic response of micronic metallic woven materials via macro-scale uniaxial tensile tests, and shows that a homogenous orthotropic constitutive model may be employed to describe the macro-scale elasticity of this class of materials with reasonable accuracy.

Keywords Orthotropic constitutive modeling · Digital image correlation · Poisson's ratio

Introduction

As composite materials continue to become more prominent in textile engineering applications, woven fiber geometries are emerging as ideal reinforcing materials. While woven materials show great potential in composites and other applications, a thorough understanding of their governing mechanics is still evolving. While several researchers have contributed to the study of fabric behavior both experimentally in the form of mechanical testing [1–6], and numerically via the Finite Element Method (FEM) [4–9], previous work often stops short of defining the elastic stiffness matrix of the subject material. Several reasons are cited for the lack of elastic constitutive modeling present in literature for this class of materials, most notably including the need to make continuum assumptions in order to formulate Hooke's Law, and the inherent difficulty present in physical strain measurements in woven geometries. It has been shown in the recent literature [3, 5, 10] that introduction of a continuum assumption for finely woven fabrics is reasonable, and is quite useful in higher order constitutive modeling of woven textiles. This work employs a homogenization assumption to model a 325× 2300 twill dutch woven wire mesh as a thin orthotropic elastic continua, where the elastic constants are regarded as averaged mechanical properties through the thickness of the structure.

The mechanical testing approach employed in this research is the uniaxial tensile test. The ASTM standard D4964 (2008) [11] gives guidelines for the tension testing of elastic fabrics. These tests are performed in the main weave directions and at intermediate orientations in intervals of 15° using a Constant Rate of Extension (CRE) type control. Off-axis tensile testing subjects the woven material to bi-axial plus shear type conditions, enabling the characterization of the yield envelope [3, 5], and estimation of shear properties [3, 12]. Any direct strain measurements must be conducted via non-contact methods to ensure that the material response is unaffected.

As is often the case with composite materials, fabrics pose a challenge in the definition of mechanical properties due to their inhomogeneous structure. Optical strain measurement techniques, including Digital Image Correlation (DIC), have

S.M. Kraft · F.A. Moslehy · Y. Bai · A.P. Gordon (✉)
Department of Mechanical and Aerospace Engineering, The University of Central Florida, Orlando, FL 32816-2450, USA
e-mail: apg@ucf.edu

emerged as the optimal method for the problem of strain measurement in reinforced composites, but research formally validating the DIC method for un-impregnated fabrics is lacking. Digital Image Correlation is a variant of the classical laser speckle techniques, which allows for the substitution of a painted speckle pattern and Charge-Coupled Device (CCD) camera in place of the more complex optical setup required for speckle interferometry. A series of images is captured in succession, starting with the un-deformed image and proceeding until the test is completed. As the specimen is deformed, the painted speckle pattern deforms with it, and this information is captured on the CCD in the form of pixel position and respective light intensity. In raw form, this generates a matrix of gray-scale values corresponding to the random speckle pattern on the specimen. As the target feature (speckle) moves in the frame onto new pixels, gray-scale values shift with it in the matrix, and this information is recorded. Digital Image Correlation has been shown to be an effective method for obtaining full-field strain measurements in woven composite materials [13], and was used successfully by Hursa and coworkers to identify the Poisson's ratio of plane and twill woven cotton fabrics of significantly less mesh density than the subject material of the current study [14]. The principal difficulties in the application of DIC to characterize woven materials is the propensity for stiffness addition caused by the application of the necessary speckle coatings, and the potential inhomogeneity of the macroscopic strain fields associated with this class of materials. The work presented herein is intended to show that DIC strain measurement is applicable to finely woven micronic wire mesh materials by demonstrating that the speckle coating process has minimal effect on the tensile response, and by leveraging full-field DIC results to establish the general homogeneity of the strain fields in the gage section of a common flat uniaxial tensile specimen. Moreover, this work is intended to establish a well-documented and repeatable test setup as a basis for the expanded use of this method in characterizing this class of materials.

This paper presents work done to experimentally define the in-plane, orthotropic, elastic constants of a stainless steel 316 L twill dutch woven wire mesh, illustrated in Fig. 1(a) and (b). Uniaxial tensile experiments, performed in various material orientations, are used to develop the orientation-dependence of the stiffness of this woven structure. Strain is measured via DIC using a high-resolution CCD camera and commercially available correlation software from Correlated Solutions, Inc.. The resulting measurements show that the strain fields in the gage section are relatively homogenous, allowing for the calculation of the homogenized orthotropic compliance for the subject material. Finally, constitutive modeling is employed to estimate the shear properties of the twill dutch woven wire mesh, and statements are made with regards to the orthotropic nature of this material.

Test Material

Wire Material and Weave Geometry

The material of interest in this study is a 325×2300 micronic twill-dutch woven wire mesh. This material is frequently used in fine filtration applications where it is exposed to biaxial loads in the form of hydrodynamic pressure, as well as temperature gradients and particle deposition. Recently, this material has been employed in explosive trace detection (ETD) applications in which it is simultaneously exposed to extreme temperature gradients and hydrodynamic forces. The mesh is woven from austenitic Cr-Ni-Mo stainless steel 316 L (SS316L) wires, giving it superb tolerance to thermal shock and repeated loading cycles. The material properties of AISI for bulk SS316L are provided in Table 1 [15]. It is noted, however, that material strength in stainless steel wires tends to increase with decreasing diameter, i.e.,

$$S_{ut} = Ad^{-m} \tag{1}$$

where A and m are material properties, and d is the wire diameter [16]. Figure 2 shows experimental results documenting the trend in strength with wire diameter [17], along with a regression fit of equation (1). In the case of room temperature SS316 wires, A is given as 145.43 ksi-in^m (1623.7 MPa-mm^m), while m is 0.149. Austenitic stainless steel wires on the order of 0.010 in. (0.254 mm) in diameter have tensile strengths as high as 275 ksi (1,896 MPa). The wires making up the woven mesh in question are of the order of one thousandth of an inch (25.4 microns) in diameter, resulting in wire strengths significantly higher than listed in Table 1. A thorough literature review yielded no similar models for yield strength of wires drawn from ferrous metals, and it is not customary for wire manufacturers to specify yield strength explicitly.

The SS316L wires are woven into the mesh in a twill-dutch pattern. This weave pattern produces an extremely dense mesh, with nominal and absolute pore sizes of 2 and 7 microns, respectively. It is assumed that the warp (toe) wires are initially un-crimped, and that all wires are in a damage free state prior to loading. The warp wire weave direction is referenced as the 0° material direction in this study, while the weft (shute) wire weave direction is referred to as the 90° orientation. Figure 1 illustrates the woven wire mesh in both micro (Fig. 1(c)), and macroscopic perspectives (Fig. 1(d)), and all key dimensions are summarized in detail in Table 2. The ASTM standard E2016 (2006) [18] provides the equations used to arrive at the reported weight values for the mesh, and the reported thickness is based on manufacturer specifications of the material.

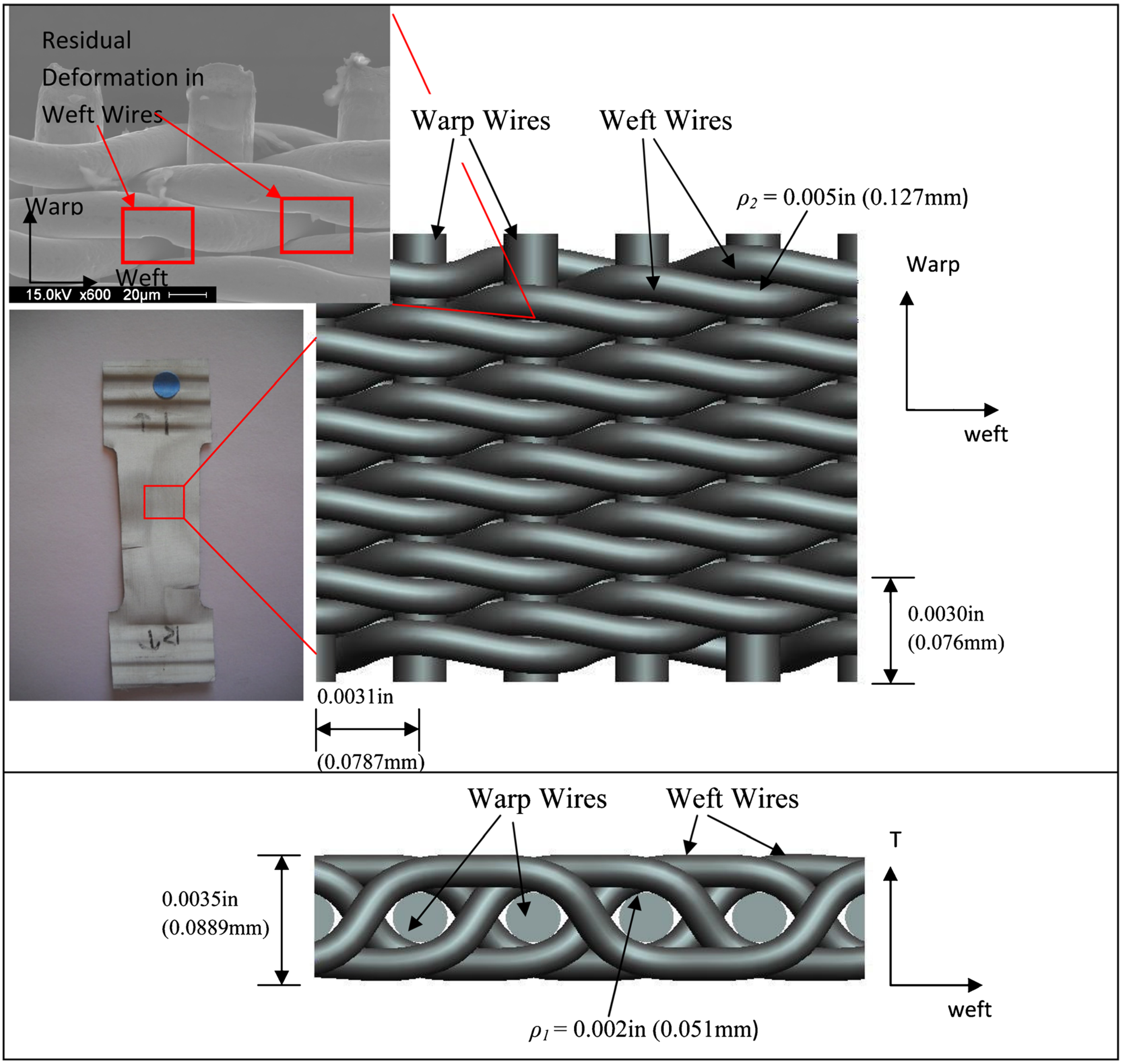

Fig. 1 Images and rendering of the 325×2300 SS316L twill dutch woven wire mesh specimen and weave geometry outlining key dimensions, and the principle material orientations referred to as the warp (w) and weft (s) directions

The Orthotropic Thin Sheet Assumption

The mechanical response of a woven wire mesh at the meso-scale is multifaceted and complex, with factors such as crimp interchange, wire sliding, wire binding, and wire tensioning all occurring simultaneously and dependently. Comprehensive mechanical analysis at the wire level quickly becomes unwieldy, and so an assumption that allows for the analysis of

Table 1 Material properties of bulk stainless steel 316 L at room temperature [15]

Units	Elastic modulus, E	Yield strength, σ_y	Ultimate tensile strength, S_{ut}	Density, ρ	Elongation, ε_f (%)	Poisson's ratio, ν	Shear modulus, G
SI	193 GPa	205 MPa	520 MPa	0.008 g/mm^3	40	0.28	75.4 GPa
English	28.0 Msi	29.7 ksi	75.4 ksi	0.289 lbf/in^3	40	0.28	10.94 Msi

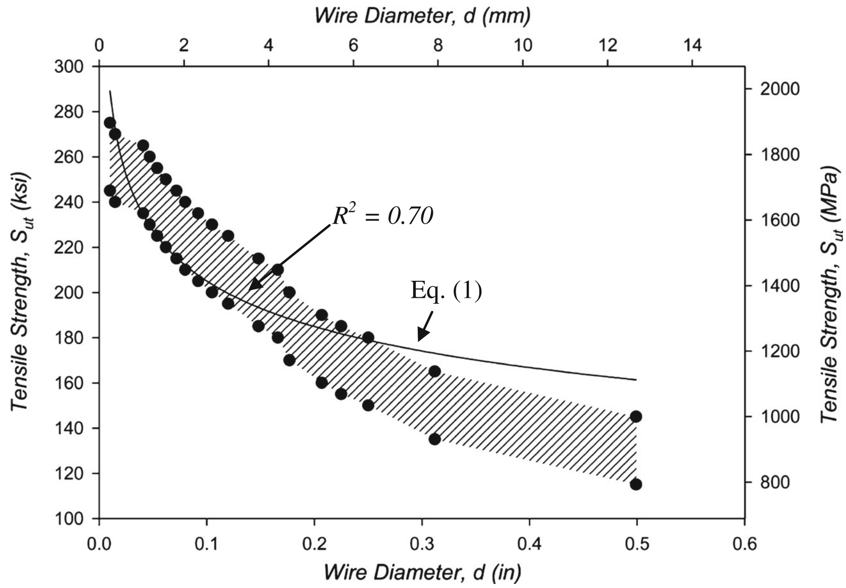

Fig. 2 Experimental and modeled tensile strength of SS316 based on wire size, and a regression fit by means of equation (1) used to produce the supplied constants A and m [20]

the material at the macro level is ideal. The assumption of homogeneity enables these materials to be modeled with a simplified orthotropic constitutive model. An orthotropic material may be defined as any material that possesses three mutually orthogonal planes of symmetry, which in general allows for the number of independent elastic coefficients to be reduced to nine. Most in-plane woven wire mesh materials possess two distinct and perpendicular weaving directions, referred to as the warp and the weft. The respective wire directions often possess their own distinct material properties due to differences in wire arrangement, size, density, processing, etc. Taking advantage of this wire configuration allows for the assumption that in-plane orthogonally woven geometries behave as thin orthotropic sheets under plane stress. The assumption of plane stress allows for further reduction of the independent elastic constants from nine to four, resulting in the simple in-plane orthotropic compliance relationship given as,

$$\begin{bmatrix} \varepsilon_w \\ \varepsilon_s \\ \gamma_{ws} \end{bmatrix} = \begin{bmatrix} \frac{1}{E_w} & \frac{-\nu_{ws}}{E_s} & 0 \\ \frac{-\nu_{ws}}{E_w} & \frac{1}{E_s} & 0 \\ 0 & 0 & \frac{1}{G_{ws}} \end{bmatrix} \begin{bmatrix} \sigma_w \\ \sigma_s \\ \tau_{ws} \end{bmatrix} \tag{2}$$

where, E_w and E_s are the elastic moduli in the warp and weft (shute) directions respectively, and G_{ws} is the in-plane shear modulus. Of the two Poisson's ratios, ν_{sw} and ν_{ws}, only one is independent due to symmetry. Poisson's ratio is a fundamental elastic material property that describes the ratio of transverse contraction to axial dilatation as given by,

$$\begin{aligned} \nu_{ws} &= -\frac{\varepsilon_s}{\varepsilon_w} \\ \nu_{sw} &= -\frac{\varepsilon_w}{\varepsilon_s} \end{aligned} \tag{3}$$

Here, the first subscript is understood to indicate the loading axis, so for the case of ν_{ws}, ε_w is the axial strain in the warp (0°) orientation, while ε_s is the transverse strain exhibited by the material in the weft (90°) direction upon uniaxial loading in the warp (0°) direction. Any out-of-plane strain in the thickness (T) direction is ignored in this work. A relationship between two Poisson ratios and the two elastic modulus is given by the following equation.

$$\frac{\nu_{ws}}{E_w} = \frac{\nu_{sw}}{E_s} \tag{4}$$

Uniaxial Tensile Experiments

Digital Image Correlation for Strain Measurement

Digital Image Correlation (DIC) is a widely used optical strain measurement technique first developed by Peters and Ranson

Table 2 325×2300 316 L SS woven wire mesh specifications

Units	Warp wire count, N_s	Weft wire count, N_w	Warp wire diameter, D_s	Weft wire diameter, D_w	Mesh thickness, T	Mesh weight, W
SI	127 *wires/cm*	905 *wires/cm*	0.0381 *mm*	0.0254 *mm*	0.0889 *mm*	483.4 g/m^2
English	325 *wires/in.*	2300 *wires/in.*	0.0015 *in.*	0.0010 *in.*	0.0035 *in.*	0.099 lb/ft^2

in the early 1980's [19]. The method is far less optically demanding than other experimental techniques such as laser speckle photography, and does not require an isolation table. White light is sufficient to illuminate the specimen. A sketch of the DIC setup used in this investigation is illustrated in Fig. 3(a). To capture the images for correlation, a high-resolution (2448×2048) CCD camera with a Tokina AT-X Pro D M100 F2.8 lens was placed on a fully leveled Velbon GEO N840 tripod centered in front of the specimen. The camera recorded images at a rate of 0.5 Hz throughout the duration of the test. Correlation of the DIC images was accomplished via a commercially available algorithm, Vic - 2D version 2009, with care being taken to assure the system was properly calibrated. In general, DIC requires the generation of a random speckle pattern directly on the surface of the test sample. The speckle pattern must be of sufficient contrast to the surface of the specimen to generate detectable gray scale value gradients across the specimen, and the speckle size must be sufficiently small as to obtain a reasonable resolution. Vic - 2D makes use of several user imputable parameters to control the computation the strain from the measured displacements. Parameters such as gray value interpolation, the correlation criterion, the subset weights, and the image filtering all effect the calculation of the strain values [20]. For the work presented herein, the gray value interpolation, which seeks to provide sub-pixel resolution by means of a continuous spline, is set as "optimized 8-tap", which provides for maximum accuracy. The correlation criterion utilized is a

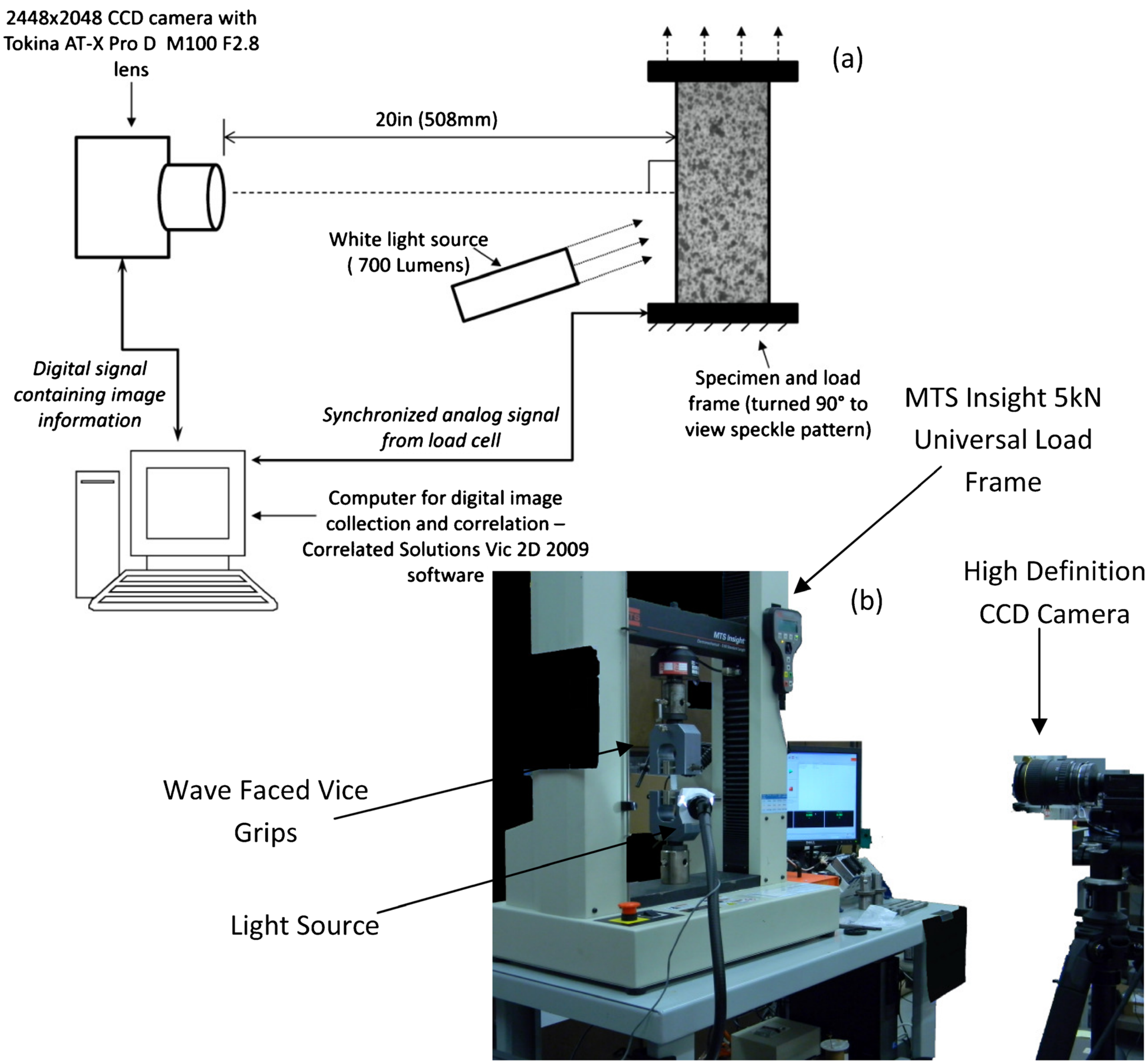

Fig. 3 (a) Diagram, and (b) photograph of the experimental setup used for Digital Image Correlation of the woven wire mesh specimens normalized squared difference method, which is generally insensitive to lighting differences between the reference and deformed images. A Gaussian subset weight parameter was employed in the correlations, which causes the subsets to be center weighted, and is conducive to maximum spatial and displacement resolution. Also, all strain results are averaged via a center weighted Gaussian filter, with a filter box size of 15 data points, which corresponds to a length of 0.03 in (0.76 mm) on the specimen.

Tensile Specimens

The woven wire mesh specimens are incised by hand from larger material sheets [144.0 in^2 (0.092 m^2)] supplied by TWP Inc., into the standard flat tensile specimen shape as per ASTM Standard E8 (2004) [21]. The flat tensile specimens have been iteratively designed to ensure optimal failure in the gauge section of the specimen, and this is the case in the majority of the experiments. The optimal flat tensile test specimen geometry is provided as Fig. 4 with a gauge width of 0.75 in. (19.05 mm.) and a gauge length of 1.25 in. (31.75 mm.). The gage section geometry produces an active (load bearing) wire count of 243 warp wires in the warp (0°) orientation, and 1,725 weft wires in the weft (90°) orientation. As the specimen orientation diverges from the main weave axes, edge effects due to wire cut-off are unavoidable. This problem is most pronounced in the 45° orientation, where a typical aspect-ratio flat tensile specimen could potentially have no wires that run the entire gauge length. The authors have given much attention to the effects of widening the test specimens to reduce edge effects in a previous work [5], with

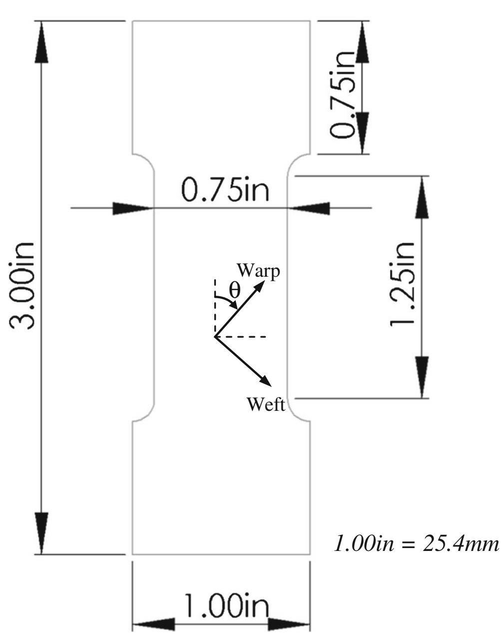

Fig. 4 Dog-bone test specimens used in uniaxial tensile experiments conducted on the 325×2300 SS316L twill dutch woven wire mesh

particular focus on how the elastic modulus and yield strength vary with orientation. From this work, it has been shown that widening the sample by a factor of two does not greatly improve test results. In fact, adverse boundary conditions that arise in clamped off-axis specimens due to shear coupling [22] are exasperated by reducing the aspect ratio of the specimens, causing failures near the specimen grips, and specimen twisting during the experiments.

Incision of the test samples by hand inherently introduces variability into the specimen geometry that could ultimately influence test results. To gauge the level of variability in these experiments arising from, amongst other possible factors, sample geometry, a series of ten tensile tests were conducted in prior work [5] on flat tensile warp (0°) specimens. In general, yield strength and stiffness showed the most notable standard deviations in normalized data, with values of 0.04, and 0.10 respectively. In general, the specimen variance was found to be small, and considered within statistical error limits for mechanical testing of this class of materials. Detailed discussion of these results is beyond the scope of this paper, and the reader is referenced to the previous work [5] for more information.

Uniaxial Tensile Results

Upon careful incision of the test specimens from the as-received sheets, a regimen of uniaxial tensile tests were performed on the subject material. The specimens were held in the load frame by wave-shaped mechanical vice grips, i.e., Test Resources Model No.G240G, suitable for gripping the very thin material samples. The flat tensile specimens were incised in both the warp (0°) and weft (90°) material orientations, and in intermediate orientations at 15° intervals as illustrated by Fig. 4. This approach produces information on the orientation dependence of material properties such as yield strength and stiffness, and allows for the application of constitutive models to the material through regression analysis or other means [3, 5, 12]. All tests were run using a MTS Insight 5 kN electromechanical uniaxial testing machine, shown in Fig. 3(b), employing a Constant Rate of Extension (CRE) type displacement control at a rate of 0.05 in/min (1.27 mm/min). All tensile tests incorporated DIC strain measurements for accurate accounting of the tensorial specimen strains in the gage section. The mechanical response of the 325×2300 SS316L woven wire mesh in various material orientations is provided in Fig. 5. Several material properties for the as-received woven wire mesh have been established from the experimental data, and these properties are defined in Table 3, where the values have been normalized by the warp (0°) direction results[a].

While the elastic response of some off-axis material orientations shown in Fig. 5 are not exactly linear in appearance, particularly the 60° case, R^2 values obtained from linear least

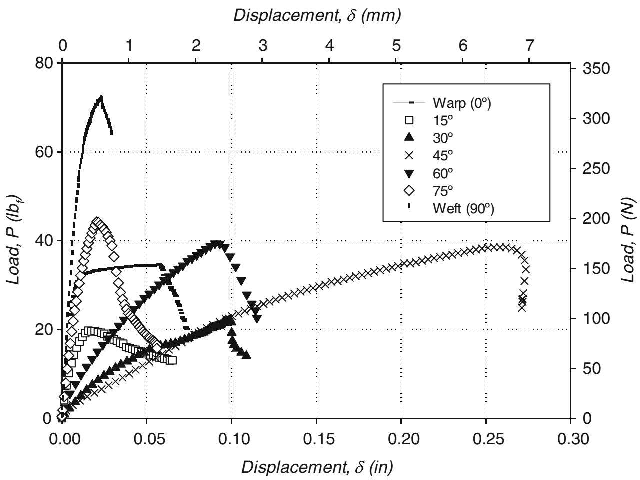

Fig. 5 Mechanical response of the 325×2300 SS316L twill dutch woven wire mesh at various material orientations with displacement measured via DIC with an initial gage length of 0.37 in (9.40) mm

squares regression fits are consistently higher than 0.9, indicating that a linear assumption is reasonable. Thus, the elastic modulus of the subject material in the various material orientations can be obtained from the tensile responses shown in Fig. 5. The values of E_w (warp) and E_s (weft) are concluded to be 3.09 Msi (21.3 GPa) and 2.88 Msi (19.9 GPa), respectively. Clearly, these values are significantly less than bulk SS316L, which is reported in Table 1 as 28.0 Msi (193.0 GPa). If we define density of the subject material in terms of area, as provided in Table 2, the specific modulus takes on values of $4.5 \times 10^9 \frac{in}{s^2}\left(11.43 \times 10^{10} \frac{mm}{s^2}\right)$ and $4.2 \times 10^9 \frac{in}{s^2}\left(10.67 \times 10^{10} \frac{mm}{s^2}\right)$ for the warp (0°) and weft (90°) orientations, respectively. This is compared to a specific modulus value for planar SS316L of $2.8 \times 10^{10} \frac{in}{s^2}\left(7.11 \times 10^{11} \frac{mm}{s^2}\right)$, calculated using the density provided in Table 1.

Table 3 Normalized tensile properties of SS316L woven wire mesh at various material orientations

Orientation, θ (°)	Stiffness, K/K_w [a]	Yield strength, $S_y/S_{y,w}$	Ultimate tensile strength, $S_{ut}/S_{ut,w}$	Fracture strength, $S_f/S_{f,w}$	Elongation, $\varepsilon_f/\varepsilon_{f,w}$
0° (Warp)	1.000	1.000	1.000	1.000	1.000
15°	0.37	0.53	0.59	0.40	0.63
30°	0.07	0.33	0.67	0.44	1.60
45° (Bias)	0.04	0.44	1.16	1.23	4.60
60°	0.18	0.75	1.19	1.27	1.50
75°	0.54	1.22	1.37	1.42	0.53
90° (Weft)	0.92	2.00	2.15	2.3	0.41

[a] K_w=6.48 kip/in (1134.8 kN/m), $S_{y,w}$=11.4 ksi (78.6 MPa), $S_{ut,w}$= 12.7 ksi (87.6 MPa), $S_{f,w}$=11.9 ksi (82.0 MPa), and $\varepsilon_{f,w}$=0.048 in/in (or mm/mm)

Characterization of the In-Plane Orthotropic Elastic Constants

The Effect of Speckle Coating on the Tensile Response

Once properly incised, each DIC specimen must be coated with a layer of flat white paint such that the entire gage section color is uniform. A speckle pattern is then placed on each gage section via a black spray paint, as shown in Fig. 6(a), with speckle diameter on the order of 0.008 in (0.20 mm). The application of the paint coating results in only a minimal increase in specimen thickness, measured at 1.00×10^{-4} in (2.54microns). It is necessary, however, to insure that the application of paint to the woven mesh specimens does not alter their mechanical stiffness. Figure 7 shows comparisons of the mechanical response of the coated and un-coated specimens in the warp (0°), bias (45°), and weft (90°) orientations. Inspection of Fig. 7 reveals that the application of the speckle coating has no significant effect on the elastic response of the woven wire mesh in the principal material orientations. The observed increase in the bias (45°) orientation stiffness upon coating is 9.6 % with respect to the uncoated specimen, which is within the range of experimental scatter observed from multiple tests in this material orientation. Thus, it is concluded that DIC strain measurements can be performed on this class of materials without significant alteration of their tensile response.

Full Field Strain Contours

Strain measurement using optical extensometry techniques is of great value to elastic property determination for the SS316L twill dutch woven wire mesh; however, the accuracy of the data extracted along a line in the gage section is dependent on the uniformity of the strain distribution in the region. To investigate the uniformity of the strain fields in the gage section, the full-field capabilities of DIC can be leveraged to plot the strain distributions. Uniformity of the strain fields also has implications on the applicability of cutting edge characterization techniques, such as the Finite Element Model Updating Method (FEMU) and others [23, 24], which could potentially be employed in future work. Figures 8 and 9 show the DIC measured strain fields in the x and y camera axes, respectively, for all experimentally treated material orientations. Note that the strain distributions in both the x and y camera axes are relatively uniform, particularly in the areas of interest outlined in Fig. 6(b). The anisotropy of the material becomes clear upon inspection of both Figs. 8 and 9, where clearly defined strain contours develop along the main load bearing material axis. The material clearly exhibits a Poisson's effect, with areas of maximum negative transverse strain coinciding with areas of maximum axial strain. The effects of load-bearing wire cut-off are made clear in Fig. 9, where the

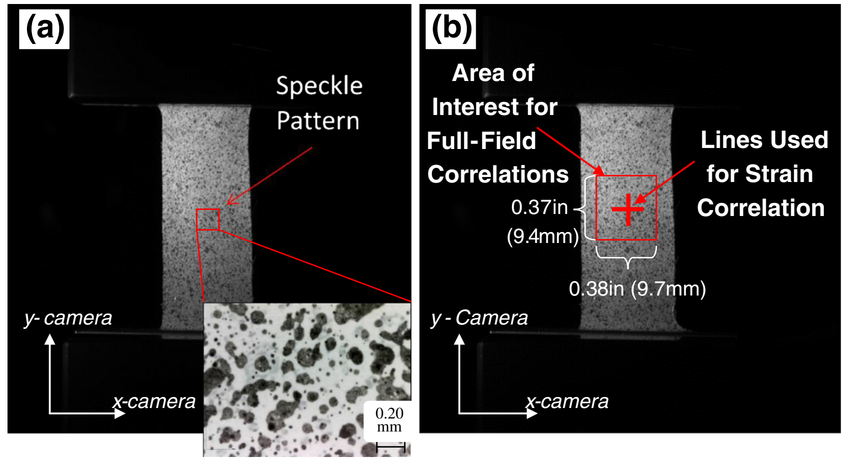

Fig. 6 (**a**) Image of the painted speckle pattern used for correlation (**b**) Illustration of the linear regions used to correlate the specimen displacements and calculate the axial and transverse strains

30° and 60° DIC *y-camera* axis strain contours show narrow bands of uniformly loaded material, corresponding to the section of wires in the specimen running the full gage length. These zones of uniform *x-camera* and *y-camera* strains delineate regions of homogenous macro-scale deformation where optical extensometry can be employed to measure average strains, and subsequently calculate the elastic constants, with minimal error. Hence, the conclusion drawn from

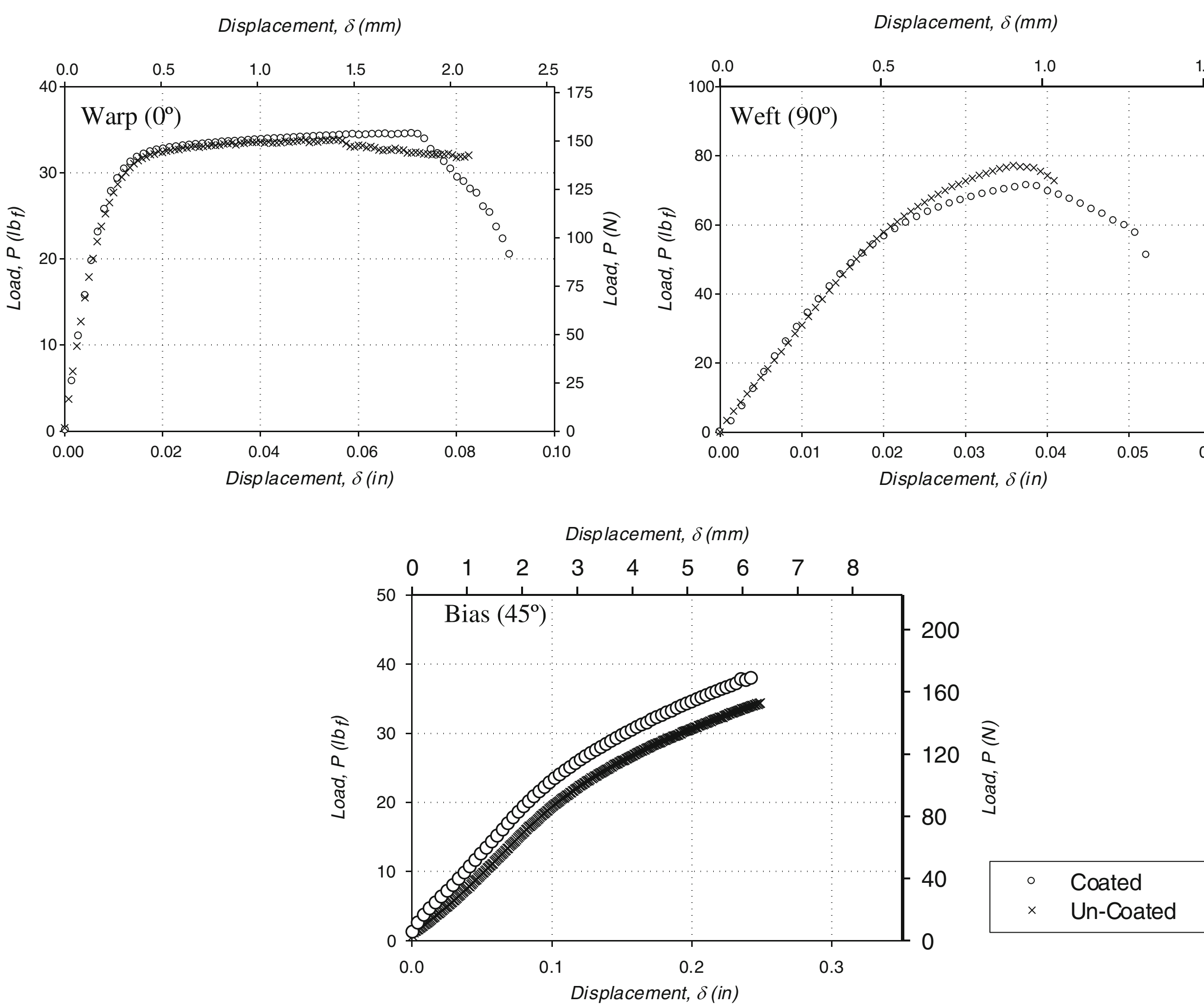

Fig. 7 Comparison of the tensile response of SS316L 325×2300 twill dutch woven wire mesh in both as received and speckle coated states

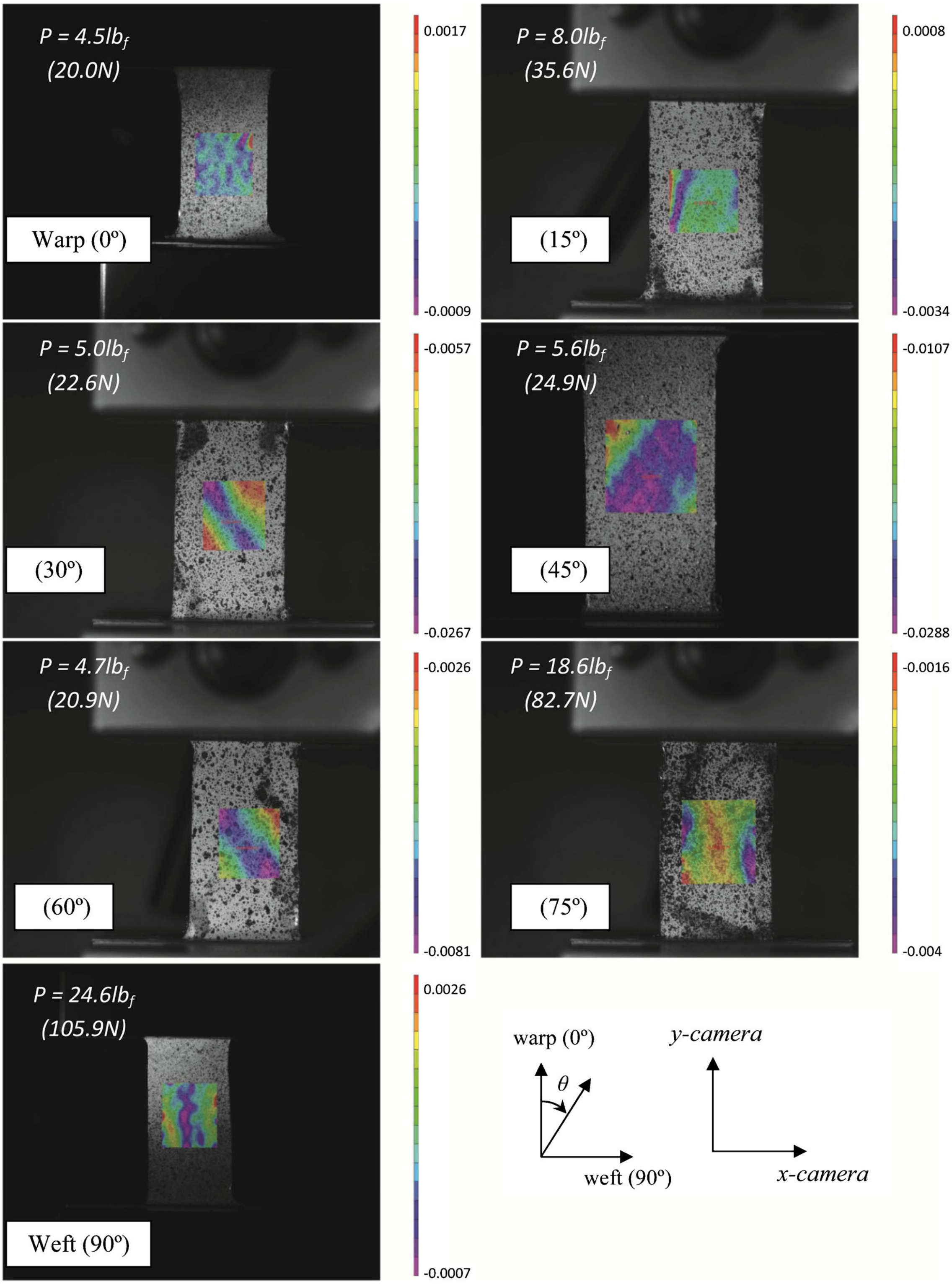

Fig. 8 Strain contours in the *x-camera* axis from testing on the woven wire mesh in various material orientations

Figs. 8 and 9 is that proceeding with strain measurements averaged over the linear regions outlined in Fig. 6(b) is reasonable for the purpose of elastic constant calibration for the SS316L woven wire mesh material.

Determination of Poisson's Ratio

As this material is being treated as a thin orthotropic sheet, it is necessary to analyze the strain developed upon loading in both

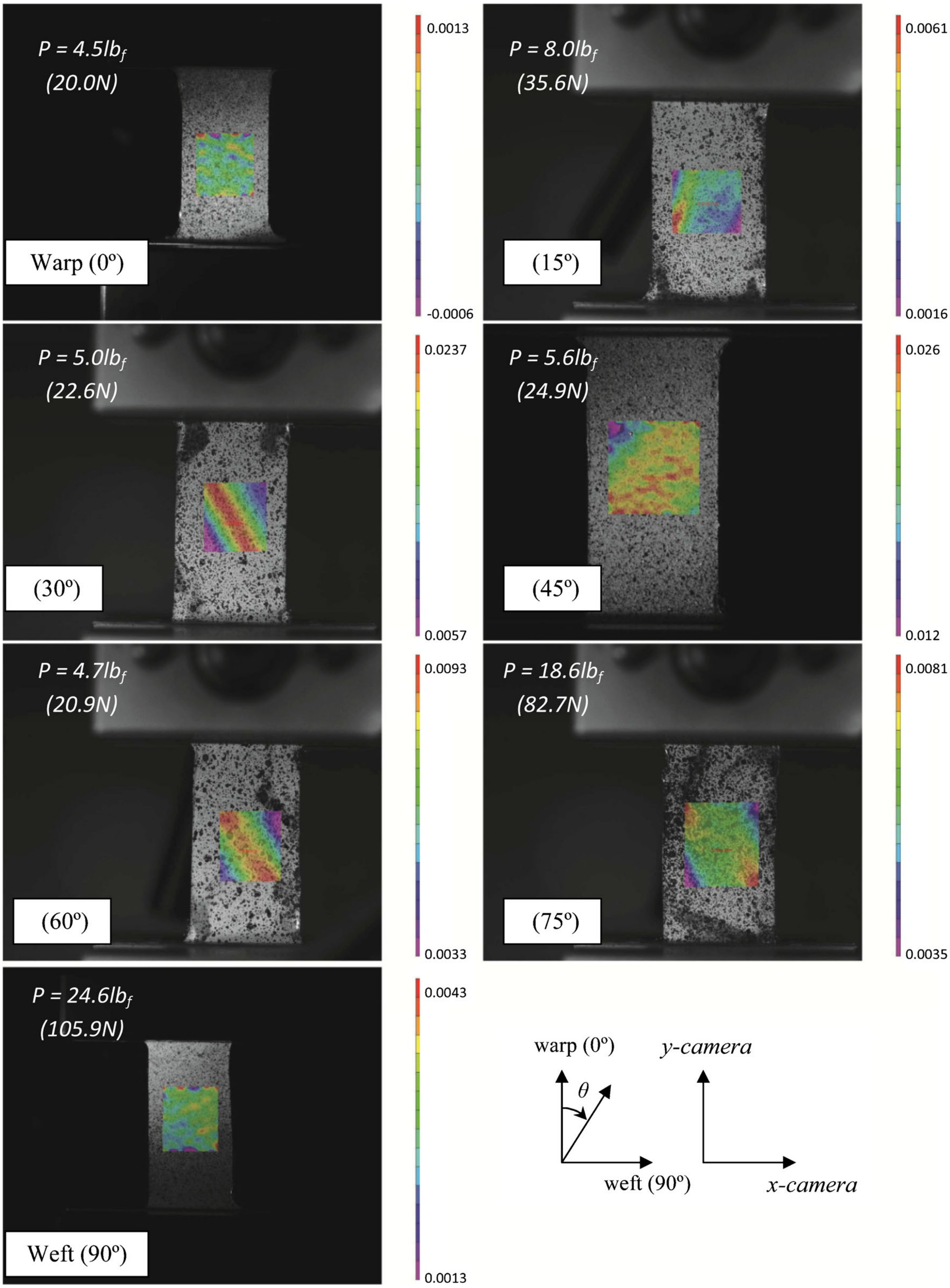

Fig. 9 Strain contours in the *y-camera* axis from testing on the woven wire mesh in various material orientations

the warp (0°) and weft (90°) orientations. This information was extracted from the DIC data via line correlation of the displacement, as illustrated in Fig. 6(b). The use of line extensometry to calculate the Poisson's ratios of the subject material reduces the amount of raw data, and serves to simplify data reduction. The length of the lines used for these correlations was guided by inspection of the full-field strain contours for each respective material orientation shown in Figs. 8 and 9, such that data was taken in the homogenous strain zones only. The process of identifying the homogenous region for strain measurement via line correlation was done individually for each orientation by inspecting the gradient of the strain across the region of interest. Strain data outside of the homogenous zone was simply omitted from the analysis, ensuring accurate calibration of the elastic constants. The results of this analysis for the principal material orientations are presented in Fig. 10, where strain is plotted with respect to the applied crosshead displacement. Analysis of Fig. 10 reveals excellent linear strain correlations in both of the axially measured directions, but considerable noise in the transverse strain correlations. It is postulated that this noise is due to the inhomogeneous structure of the material. In monolithic materials, strain energy is transmitted throughout the microstructue by intergranular bonding forces which are relatively strong. These intergranular forces allow for smooth strain distributions throughout the material, and even distribution of load from remote displacements. In the case of woven wire materials, load is transmitted throughout the structure by discrete wires, and inter-wire forces, i.e., friction, are relatively weak. As such, the transverse contraction of the mesh is considerably less uniform at the meso-scale than monolithic SS316L. This discretized material response results in the somewhat erratic transverse strain progression with time. This phenomenon is dealt with in this study through an effective averaging of the transverse strain, accomplished via a linear regression fit through the data. Figure 10 shows that the linear regression coefficients for the axial strain measurements are nearly 1.0, while the regression coefficients in the transverse directions are reasonable enough to proceed with the classification of Poisson's ratio. Also, it is noted that the weft (90°) orientation transverse strain measurements appear to not pass through the origin as would be expected. This is due to a post-processing procedure necessary to correct for the presence of a non-linear strain region in the early stages of elastic loading caused by wire crimp interchange and relative sliding [4]. To account for this, the linear transverse strain values have been shifted to the vertical axis, and the slope of this curve is taken as the value to calculate Poisson's ratio. This procedure is akin to toe-compensation, which is commonly used to account for nonlinearities in low-load tensile results caused by slack in the load frame, and does not affect the calibration of the elastic constants.

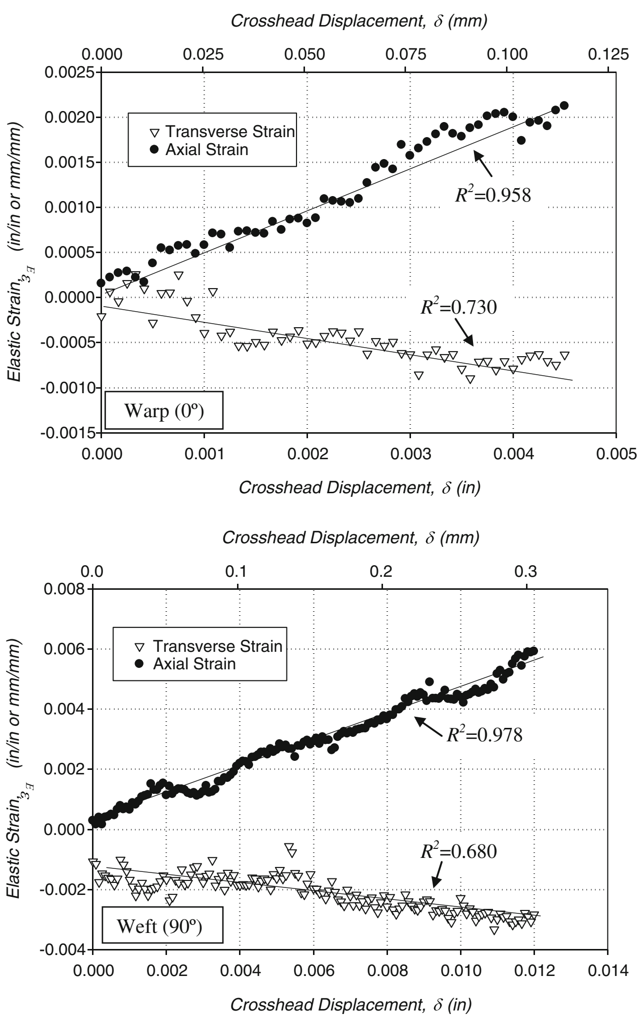

Fig. 10 Digital Image Correlation measurements of transverse and axial elastic strain in the warp (0°) and weft (90°) orientations

The Poisson's ratio of the twill dutch woven wire mesh in the warp (0°) direction, ν_{ws}, is found to be 0.398, while the value in the weft (90°) orientation, ν_{sw}, is 0.312. These values are within the range predicated by Hooke's law, and are consistent with values reported in the literature for woven materials [14]. From these strain measurements, and the associated material stiffness values, the in-plane orthotropic elastic stiffness matrix can be populated. As a means to test the assumption that this material is orthotropic, the symmetry condition of in-plane orthotropic materials must be confirmed within the margin of experimental error. In this case, the experimentally-determined Poisson's ratio and elastic moduli values can be used to show that the symmetry condition is met only to within 18.0 %, which draws into question the assumption of orthotropic behavior for this material. Indeed, inspection of the weave structure presented in Fig. 1(a) suggests that the weave may not be structurally symmetric on the meso-scale. It is clear that further experiments are required to confirm the macro-scale symmetry of this material, and to justify the use of an orthotropic constitutive assumption to model the SS316L woven wire mesh. The dependence of the fifth elastic constant for the in-plane orthotropic constitutive model employed in this work can be established via equation (4).

Off-Axis DIC Experiments

To investigate the assumption of orthotropy of the subject material further, it is necessary to consider the results from off-axis tensile experiments. In particular, it must be shown that the tensile response of the SS316L woven wire mesh is unaffected by an orthogonal transformation of the material

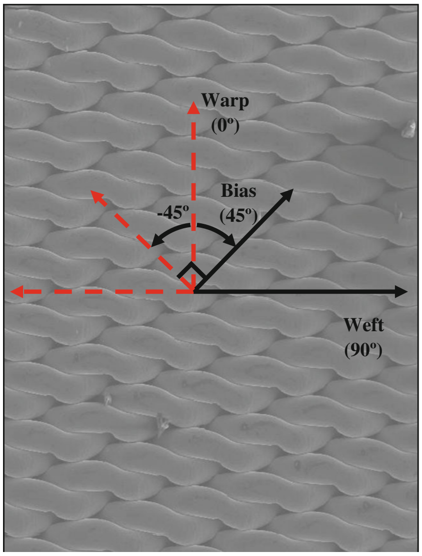

Fig. 11 Illustration of the off-axis material orientations used to test the assumption of orthotropic symmetry in the SS316L woven wire mesh material

frame. To test the assumption of macro-scale symmetry, two verification DIC experiments were conducted. These experiments were carried out on uniaxial specimens incised at 45°, and at the supplementary angle, −45°, to the specifications outlined in Fig. 4. As illustrated in Fig. 11, orthotropy of the subject material requires the elasto-plastic response in these two orthogonal axes to be consistent. The DIC results from the two orthogonal off-axis experiments have been leveraged to plot the load–displacement response of the subject material in the 45° and −45° degree material orientations. Figure 12 shows these results graphically. Emphasis should be placed on the similarity of the stiffness and the hardening response of the two orientations, suggesting that the material is in fact symmetric in-plane. This ultimately leads to the conclusion that the 325×2300 twill

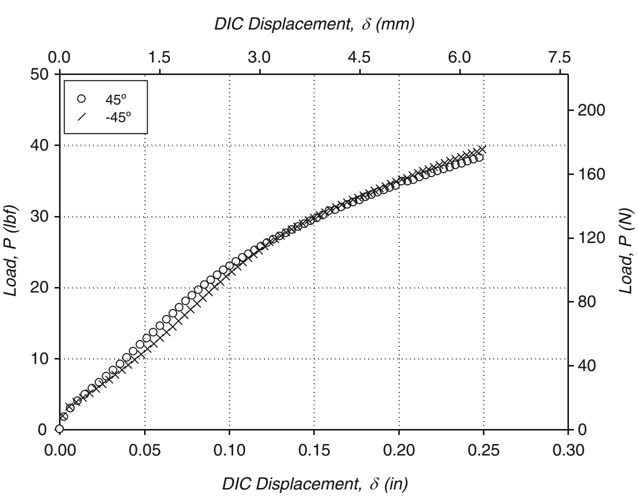

Fig. 12 The tensile response of 325×2300 twill dutch woven wire mesh in the supplementary bias orientations, measured with an initial gage length of 0.37 in (9.40) mm

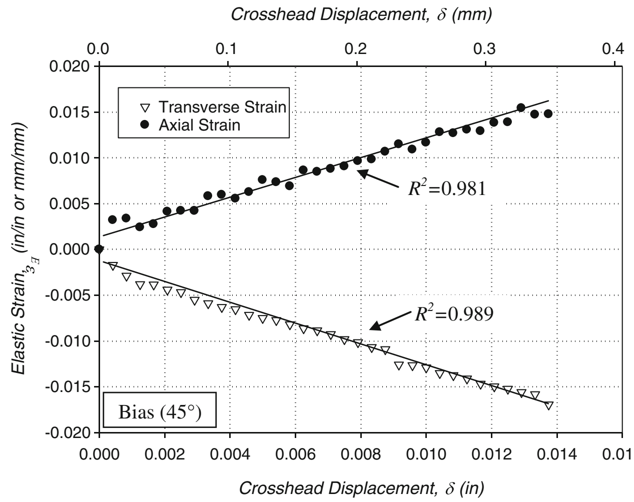

Fig. 13 Digital Image Correlation measurements of the transverse and axial elastic strain in the bias (45°) material orientation

dutch woven wire mesh is mechanically symmetric, and thus by definition may be classified as linear elastic orthotropic in-plane. Additional support for this conclusion can be drawn from the lack of shear strain observed in the principal material orientations, indicating that the addition of coupling terms to the compliance is not warranted. It is also noted that the shear strains measured in the bias (45°) material orientation are an order of magnitude smaller than the axial strains. The lack of dependence of the fifth in-plane orthotropic elastic constant is then deemed to be a result of error stemming from the assumption of continuity inherent to Hooke's law in general. It must be emphasized that the mesh orthotropy is verified only for the elastic case, and that this conclusion cannot be extended beyond the elastic limits of the material.

Previous work by has been done by the authors to investigate the ratcheting response of the SS316L woven wire mesh material [5], and it has been shown that the subject material exhibits minimal hysteresis in all experimentally treated

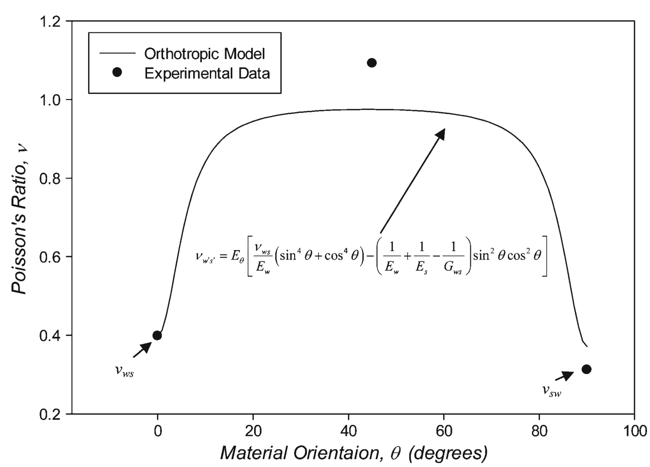

Fig. 14 Model of the orientation dependence of the Poisson's ratio of 325×2300 twill Dutch woven wire mesh in conjunction with the experimental results

Table 4 In-plane orthotropic elastic constants for SS316L 325×2300 woven wire mesh

Material orientation, θ (°)	Elastic modulus, E	Poisson's ratio, ν	Shear modulus, G
Warp (0°)	3.09 Msi (21.3 GPa)	0.398	0.031 Msi (0.214 GPa)
Weft (90°)	2.88 Msi (19.9 GPa)	0.312	0.031 Msi (0.214 GPa)
Bias (45°)	0.123 Msi (0.848 GPa)	1.09	1.08 Msi (7.44 GPa)

material orientations, and that the second loading cycle does not differ considerably from the first. Thus, it is reasonable to assume that the cyclic elastic response of the subject material may also be treated as orthotropic.

In addition to the tensile response of the ±45° material orientations obtained from DIC testing, further correlations were carried out to measure the axial and transverse strains in the 45° material orientation. It is noted that all experimental conditions and correlation procedures used for the 45° case are identical to those used for the principle material orientations. Figure 13 shows the elastic strain measurements in the 45° oriented 325×2300 twill dutch woven wire mesh as they evolved with respect to crosshead displacement. Analysis of Fig. 13 reveals that the measured transverse strain is nearly equal to the axial strain, resulting in a Poisson's ratio of 1.09 for the 45° orientation. While this value appears high, it is not unreasonable based on modeled and experimental data for woven fabrics available in literature [25, 26], with Poisson's ratio values being observed well above 0.50.

Analytical Modeling Using the In-Plane Orthotropic Assumption

As there is currently no standard governing the use of DIC methods to characterize the mechanical properties of micronic metallic woven structures, particularly via off-axis uniaxial tensile tests, it is necessary to build confidence in the experimental results through either analytical or numerical modeling. In order to give credence to the experimental results, and to further strengthen the assumption of orthotropy, an effort has been made to model the elastic properties with respect to material orientation. Such modeling can be facilitated analytically by considering a transformation through θ of the compliance matrix of a generally orthotropic sheet under conditions of uniaxial stress [22], i.e.,

$$E_\theta = \left[\frac{1}{E_w}\cos^4\theta + \left(\frac{1}{G_{ws}} - \frac{2\nu_{ws}}{E_w}\right)\sin^2\theta\cos^2\theta + \frac{1}{E_s}\sin^4\theta\right]^{-1} \quad (5)$$

$$\nu_{w's'} = E_\theta\left[\frac{\nu_{ws}}{E_w}(\sin^4\theta + \cos^4\theta) - \left(\frac{1}{E_w} + \frac{1}{E_s} - \frac{1}{G_{ws}}\right)\sin^2\theta\cos^2\theta\right] \quad (6)$$

Here, the subscripts w and s refer to the warp (0°) and weft (90°) principal material orientations, respectively, and the subscript θ is in reference to the loading direction. It is noted that similar equations exist for the other two independent elastic properties; the shear modulus and the transverse elastic modulus. It is clear from inspection of equation (5) that the bias (θ=45°) elastic modulus, obtained from Fig. 12 as 122.9 ksi (847.37 MPa), along with the already determined elastic properties from the principal material axes, can be used to solve for the shear modulus, G_{ws}, of the woven wire mesh. Furthermore, the value for G_{ws} can be used in conjunction with the other determined elastic properties in equation (6) to model the off-axis Poisson's ratio of this material. Figure 14 shows that the model predicts a value of 0.975 for Poisson's ratio in the 45° orientation, which represents a percent difference of 11.4 % from the experimentally measured value of 1.09. Table 4 provides the experimentally determined elastic modulus and Poisson's ratio values for the SS316L woven wire mesh material, along with the shear moduli derived from equation (5). As is expected for woven materials, the local in-plane shear modulus is only approximately 1.0 % of the respective tensile moduli, whereas the shear modulus of monolithic SS316L is significantly higher, approximately 35 % of the bulk tensile moduli. The low shear stiffness values observed in the principal material orientations are consistent with low energy transference between adjacent wires, with relatively weak frictional forces being the primary mechanism.

It is also of interest to utilize equation (5), referred to hereafter as the Elastic Modulus Orientation Function (EMOF), to model the off-axis elastic moduli of the woven wire mesh material. Figure 15 shows the variation in the elastic modulus with material orientation, along with the EMOF calibrated with the constants from Table 4. Note that the elastic moduli values reported in Fig. 15 are normalized by

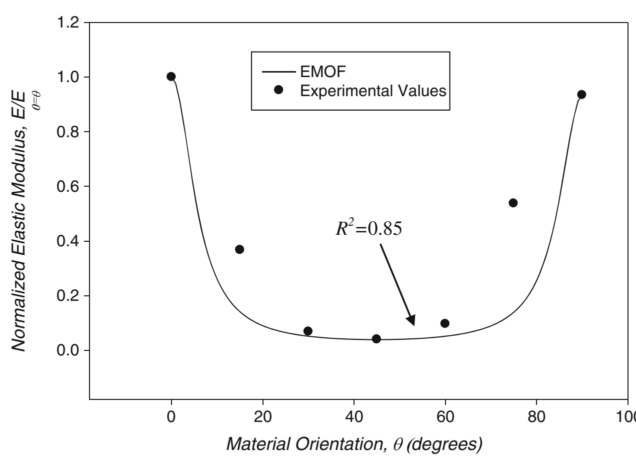

Fig. 15 The elastic modulus of the 325×2300 twill dutch woven wire mesh as a function of material orientation, along with the EMOF calibrated from DIC experimental results

the value in the warp (0°) material orientation, E_w, 3.09 Msi (21.3 GPa). Investigation of Figure 15 reveals that the EMOF fits the off-axis elastic modulus data well, with an R^2 value of 0.85. Thus, it is concluded that the experimental and modeling efforts employed in this study have produced good results, and that use of an in-plane orthotropic constitutive model to relate stress and strain in macro-scale SS316L woven wire mesh is within reason.

Conclusions

The uniaxial tensile test, incorporating a DIC strain measurement apparatus, has been identified as a viable experimental technique for the identification of the macro-scale elastic constants of a 325×2300 SS316L twill dutch woven wire mesh material. It has been demonstrated that the addition of a painted speckle coating to the un-impregnated metallic woven structure does not significantly alter the mechanical properties of the mesh. Furthermore, full-field DIC has been leveraged to investigate the homogeneity of the strain fields in the gage section of the test specimens, and the results show that regions of fairly homogenous strain exist, justifying the use of averaged strain results from optical extensometry to calculate the elastic properties of the subject material. A constitutive model has been used to formulate an estimate for the shear modulus of the 325×2300 woven wire mesh based on off-axis tensile results, and the shear modulus of this material has been shown to be markedly lower than the respective tensile moduli, indicative of low energy transference between adjacent wires in the mesh. The assumption of macro-scale orthotropic symmetry of the woven wire mesh has been confirmed via both analytic modeling, and via off-axis tensile tests on orthogonally oriented tensile specimens. Ultimately, the research presented in this paper demonstrates that a DIC system can be successfully leveraged to characterize the elastic response of finely woven heterogeneous materials, and that future extension to more complex loading conditions and specimen geometries is warranted.

Acknowledgments Ali P. Gordon would like to thank CAE Link Faculty Fellowship. The authors would also like to acknowledge Mr. Yueqian Jia for his technical assistance with the DIC measurements.

References

1. Kumazawa H, Susuki I, Morita, Kuwabara T (2005) Mechanical properties of coated plain weave fabrics under biaxial loads. Trans Jpn Soc Aeronaut Space Sci 48(160):117–123
2. Zheng J, Takatera M, Inui S, Shimizu Y (2008) Measuring technology of the anisotropic tensile properties of woven fabrics. Text Res J 78(12):1116–1123
3. Chen S, Ding X, Yi H (2007) On the anisotropic tensile behaviors of flexible polyvinyl chloride-coated fabrics. Text Res J 77(6):369–374
4. Cavallaro P, Sadegh A, Quigley C (2007) Decrimping behavior of uncoated plain-woven fabrics subjected to combined biaxial tension and shear stresses. Text Res J 77(6):404–416
5. Kraft S, Gordon AP (2011) Characterization of the mechanical behavior of a metallic fiber woven structure. Text Res J 81(12):1249–1272
6. Kraft S, Gordon AP (2013) Yield characteristics of a twill dutch woven wire mesh via experiments and modeling. J Appl Mech 80(4):0410021–04100211
7. Tarfaoui M, Drean JY (2001) Predicting the stress–strain behavior of woven fabrics using the finite element method. Text Res J 71(9):790–795
8. Nicolleto G, Riva E (2004) Failure mechanisms in twill-weave laminates: FEM predictions vs. experiments. Compos A 35:787–795
9. Barbero EJ, Trovillion J, Mayugo JA, Sikkil KK (2006) Finite element modeling of plain weave fabrics from photomicrograph measurements. Compos Struct 73:41–52
10. King M, Jearanaisilawong P, Socrate S (2005) A continuum constitutive model for the mechanical behavior of woven fabrics. Int J Solids Struct 42:3867–3896
11. ASTM Standard D4964 (2008) Tension and elongation of elastic fabrics (constant-rate-of-extension type tensile testing machine). ASTM International, West Conshohocken
12. Saliklis EP, Falk RH (2000) Correlating off-axis tension tests to shear modulus of wood-based panels. J Struct Eng 126(5): 621–625
13. Lomov SV, Willems A, Verpoest I, Zhu Y (2006) Picture frame test of woven composite reinforcements with a full-field strain registration. Text Res J 76(3):243–252
14. Hursa A, Rolich T, Ercegovic 'Razic' S (2009) Determining pseudo poisson's ratio of woven fabric with a digital image correlation method. Text Res J 79(17):1588–1598
15. Blandford RK, Morton DK, Snow SD, Rahl TE (2007) Tensile stress–strain results for 304L and 316L stainless steel plate at temperature. The Proceedings of the 2007 ASME Pressure Vessels and Piping Conference. San Antonio, Texas, July 20–26
16. Budynas RG, Nisbett JK (2008) Shigley's mechanical engineering design, 9th edn. McGraw-Hill, New York
17. ASM International (1990) ASM handbook vol. 1: properties and selection: irons, steels, and high-performance alloys. ASM International, Materials Park, OH
18. ASTM Standard E2016 (2006) Standard specification for industrial woven wire cloth. ASTM International, West Conshohocken
19. Peters WH, Ranson WF (1982) Digital imaging techniques in experimental stress analysis. Opt Eng 21(3):427–432
20. Correlated Solutions (2009) Vic 2D reference manual. Correlated Solutions, Columbia
21. ASTM Standard E8 (2004) Standard test methods for tension testing of metallic materials. ASTM International, West Conshohocken
22. Gibson RF (2007) Principles of composite material mechanics, 2nd edn. CRC Press, Boca Raton
23. Avril S, Bonnet M, Bretelle AS, Grédiac M, Hild F, Ienny P, Latourte F, Lemosse D, Pagano S, Pagnacco E, Pierron F (2008) Overview of identification methods of mechanical parameters based on full-field measurements. Exp Mech 48(4):381–402
24. Drapier S, Gaied I (2007) Identification strategy for orthotropic knitted elastomeric fabrics under large biaxial deformations. Inverse Probl Sci Eng 15(8):871–894
25. Sun H, Pan N, Postle R (2004) On the Poisson's ratios of a woven fabric. Compos Struct 68:505–510
26. Boubaker BB, Assidi M, Ganghoffer JF (2010) Evaluation of Poisson's ratio of textiles from mesoscopic models. Int J Mater Form 3(Suppl 1):81–84